Large Eddy Simulations for Detailed Soot Investigations

David Sakellarakis, Daniele Farrace, Michele Bolla, Yuri Martin Wright, Konstantinos Boulouchos
Aerothermochemistry and Combustion Systems Laboratory, ETH Zurich

1 Introduction

Modelling of soot formation in diesel engines is a challenging task, because it depends on the accurate description of a long chain of complex processes such as break-up, atomization and evaporation of the liquid fuel, mixture formation, auto-ignition and combustion in a turbulent flow-field as well as the interaction of chemistry and turbulence with the soot dynamics themselves.
In this study, the spatially filtered conservation equations are solved numerically and a semi-empirical soot model is implemented in order to simulate a reacting n-dodecane spray. The simulation pertains to experiments conducted in the cube-shaped, pre-burn combustion vessel of Sandia National Laboratories[1] (**Fig 1.a)**. The corresponding computational grid, which consists of 1.8 million cells, is shown in **Fig 1.b**. The test case considered (**Table 1**) represents engine-relevant conditions with moderate EGR.

Table 1: Operating conditions for Spray A

Ambient Temperature	900 K	Injection Duration	6 ms
Ambient O_2 mol fraction	15%	Fuel Type	n-dodecane
Ambient Density	22.8 kg/m^3	Fuel Temperature	363 K
Injection Pressure Difference	150 MPa	Orifice Diameter	0.091 mm

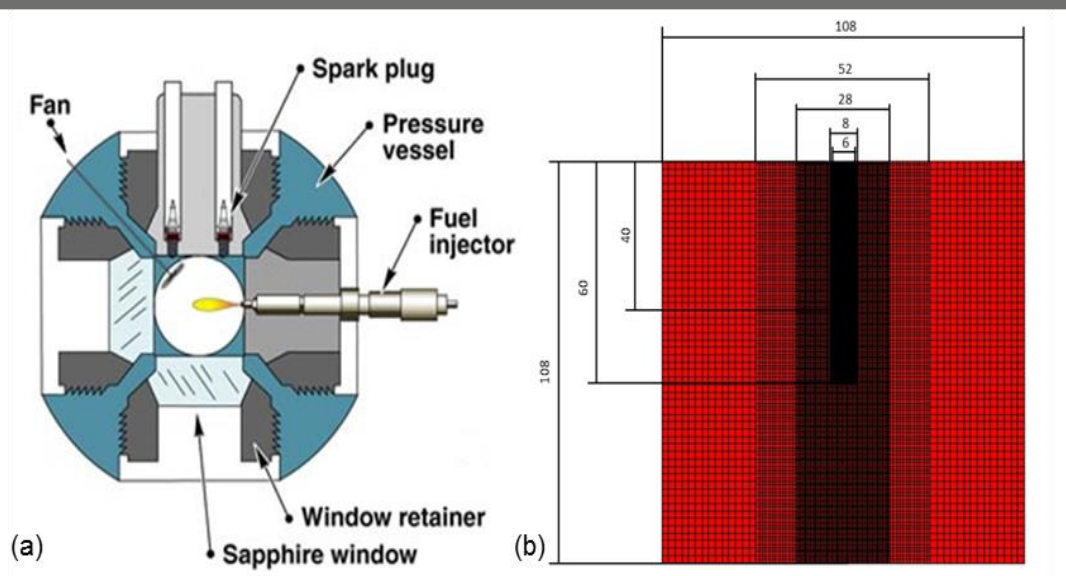

Figure 1: a) Schematic of the optically accessible high-temperature, high-pressure combustion chamber. b) Cross-section of the computational grid at the midplane of the domain.

2 The Soot Model

The two-equation model originally proposed by Leung[2] and extended by Kronenburg[3] has been employed in this study. Additional transport equations are solved for the soot mass fraction (Y_s) and particle number density (N_s). Monodisperse distribution and spherical shape are assumed for the soot particles.
The model accounts for simultaneous particle inception, surface growth by C_2H_2 adsorption, oxidation by O_2, oxidation by OH and agglomeration (**Table 2**). Accordingly, the source terms of the two equations read:

- $\omega_{Y_s} = 2R_{INCP} + 2R_{SGRW} - R_{OxO2} - R_{OxOH}$
- $\omega_{N_s} = 2R_{INCP}\, N_{AV}/n_{C,min} - R_{AG}$

The reaction rate constants in I to IV follow Arrhenius-like expressions of the form: $k = AT^{\beta}e^{-\frac{T_a}{T}}S_{soot}^{c}$. The last term represents the functional dependence of the respective process on soot surface density, S_{soot}.

Table 2: Kinetic mechanism of soot

No	Process	Reaction	Reaction Rate
I	Particle Inception	$C_2H_2 \xrightarrow{R_{INCP}} 2C_{(s)} + H_2$	$R_{INCP} = k_{INCP}[C_2H_2]$
II	Surface Growth	$C_2H_2 + nC_{(s)} \xrightarrow{R_{SGRW}} (n+2)C_{(s)} + H_2$	$R_{SGRW} = k_{SGRW}[C_2H_2]$
III	Oxidation by O_2	$C_{(s)} + {}^1/_2\, O_2 \xrightarrow{R_{OxO2}} CO$	$R_{OxO2} = k_{OxO2}[O_2]$
IV	Oxidation by OH	$C_{(s)} + OH \xrightarrow{R_{OxOH}} CO + H$	$R_{OxOH} = k_{OxOH}[OH]$
V	Agglomeration	$nC_{(s)} \xrightarrow{R_{AG}} C_{n(s)}$	$R_{AG} = 2C_a\left(\frac{6M_s}{\pi\rho_s}\right)^{1/6}\left(\frac{6k_{Boltz}T}{\rho_s}\right)^{1/6}(\rho N_s)^{11/6}$

3 Results and Discussion

Vapor penetration shows excellent agreement with the experiment, while global soot mass is underestimated by one order of magnitude (**Fig 2.a**). This discrepancy can be addressed by tuning A_{SGRW}, which has originally been calibrated for CH_4-air flames at atmospheric pressure.
The time-averaged[4] soot volume fraction contours also show a very similar distribution of sooting areas with the experiment (**Figure 2.b**). Soot presence is confined to the fuel-rich areas of the spray and downstream of the flame lift-off length, in the vicinity of which formation of C_2H_2 is favored. High intermittency is correctly reproduced.
Conceptually the soot cloud (defined as 2%$fv_{soot,max}$) can be divided in three distinct zones of soot evolution (**Figure 2.c**). The first zone extends from the onset of soot formation until the location of peak net formation. The second zone marks the transition from maximum net formation to maximum net oxidation. The last zone tracks the oxidation of soot, with inception and surface growth fading in the absence of C_2H_2, as the mixture leans out and the flame tip is approached. Particle inception contributes little to soot mass per se, but it is important for creating the sites where the bulk of formation will take place by surface growth, slightly upstream of peak soot volume fraction. O_2-oxidation takes place in a very thin layer across the flame, mostly on the fuel-rich side (see also **Fig 2.d**). OH-oxidation extends over a much wider area than O_2-oxidation because of the greater extent of OH presence in the fuel rich zone and is therefore ultimately more dominant.
Analysis of azimuthally and radially integrated quantities along the spray axis (**Fig 2.e)** yields that surface growth rate is affected more by the distribution of soot (correlation coefficient: $\langle r \rangle = 0.876$) than by the soot precursor ($\langle r \rangle = 0.651$), which is itself controlled by mixture with equivalence ratio over 1.5 ($\langle r \rangle = 0.955$). O_2 mass encompassed by the soot cloud agrees very well with O_2-oxidation $\langle r \rangle = 0.879$, even though only 40% takes place within the cloud. Finally, correlation between OH and OH-oxidation is even higher ($\langle r \rangle = 0.964$), because about 90% of soot oxidation by OH takes place within the soot cloud.
Overall, LES offers a framework capable of predicting accurately the spatial distribution of soot as well as capturing transient and intermittent processes with a simple model.

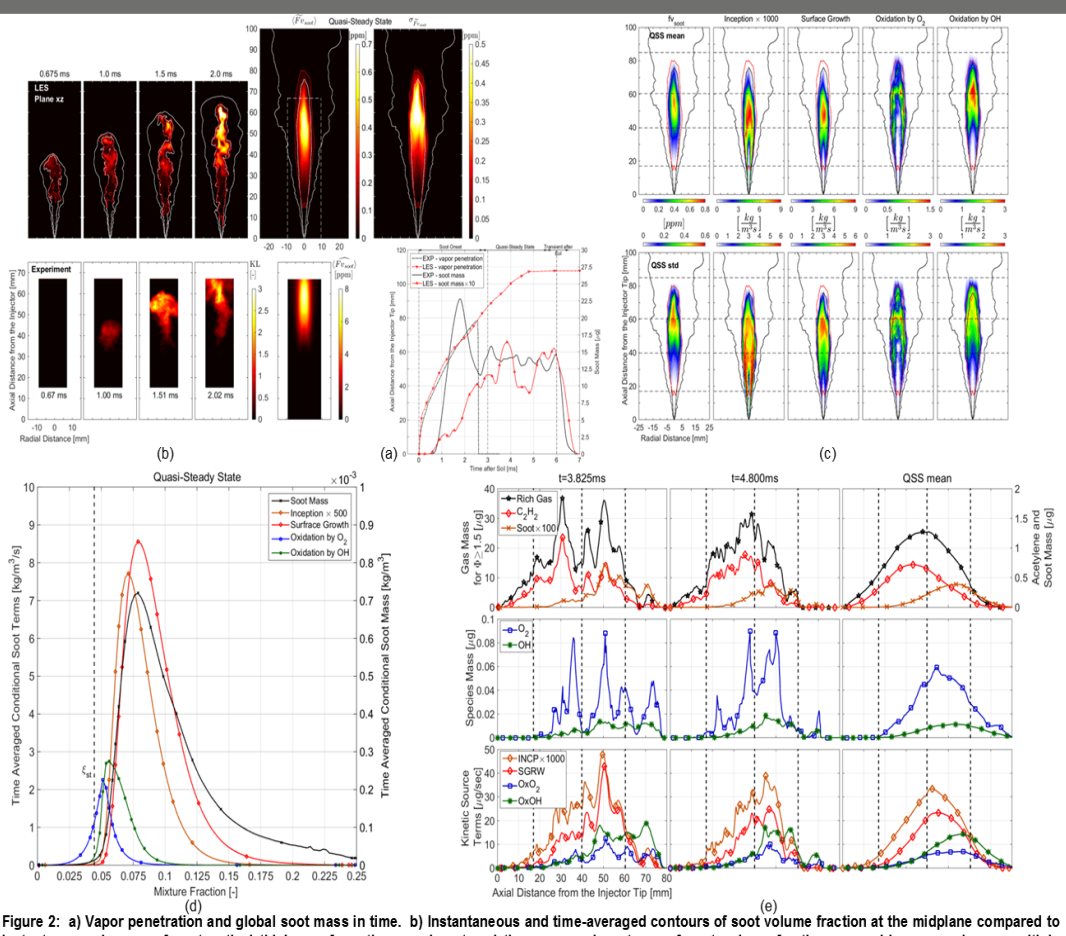

Figure 2: a) Vapor penetration and global soot mass in time. b) Instantaneous and time-averaged contours of soot volume fraction at the midplane compared to instantaneous images of soot optical thickness from the experiment and time-averaged contours of soot volume fraction, ensemble-averaged over multiple experimental realizations. c) Mean and standard deviation of soot volume fraction and kinetic terms. d) Time-averaged conditional soot terms. e) Variation of radially and azimuthally integrated quantities in 0.1mm slices along the centerline.

4 Acknowledgements

Financial support from the Swiss Federal Office of Energy (grant no. SI/500818-01) and the Swiss Competence Centre Energy and Mobility (CCEM project “ScheDual”) is gratefully acknowledged.

5 References

1. Pickett, L.M., *Engine Combustion Network.* http://www.sandia.gov/ecn/dieselSprayCombustion.php
2. Leung, K.M., R.P. Lindstedt, and W.P. Jones, *A Simplified Reaction-Mechanism for Soot Formation in Nonpremixed Flames.*
3. Kronenburg, A., R.W. Bilger, and J.H. Kent, *Modeling soot formation in turbulent methane-air jet diffusion flames.*
4. Farrace, D., et al., *Analysis of Averaging Methods for Large Eddy Simulations of Diesel Sprays.*